Proc. of the European Safety and Reliability Conference (ESREL 2026)
Edited by José C. Matos, Paulo B. Lourenço, Michael Beer, Daniel Oliveira, Edoardo Patelli, Hélder S. Sousa, Rui A. Silva and Monica Santamaria

doi: 10.3850/ESREL2026061419_esrel26-p27745-cd

Reliability-based capacity design of timber connections comprising glued-in steel plates

Aurélien Vuffray

ETH Zurich, Institute of Structural Engineering, Stefano-Franscini-Platz 5, 8093 Zürich, Switzerland.
E-mail: aurelien.vuffray@ibk.baug.ethz.ch

Alex Sixie Cao

ETH Zurich, Institute of Structural Engineering, Stefano-Franscini-Platz 5, 8093 Zürich, Switzerland.
E-mail: cao@ibk.baug.ethz.ch
Empa - Swiss Federal Laboratories for Materials Science and Technology, Structural Engineering Research Laboratory, Uberlandstrasse 129, 8600 Dübendorf, Switzerland. E-mail: alex.cao@empa.ch

Andrea Frangi

ETH Zurich, Institute of Structural Engineering, Stefano-Franscini-Platz 5, 8093 Zürich, Switzerland.
E-mail: frangi@ibk.baug.ethz.ch

Connections play a crucial role in timber structures. They not only allow the structural members to be joined together, but also govern the structure's mechanical behavior. Moreover, carefully designed connections provide ductility to the structure. Glued-in steel plates in timber are attractive in applications where high stiffness and capacity are required. To ensure the connection ductility, the steel plate should yield before brittle timber failure occurs. Thus, the design challenge lies in determining the optimal steel plate parameters that maximize the connection capacity and ensure connection ductility. In this study, system reliability is used to determine the optimal steel plate thickness based on an analytical model of the glued-in plate connection. This results in a hierarchical calibration of the failure modes to provide ductility to the system in the event of failure. The proposed framework enables the economical and robust design of glued-in plate connections, supporting their wider adoption in timber structures.

Keywords: weak link, ductility, system reliability, timber engineering, glued-in plates, reliability-based design.

1. Introduction

The construction of multi-story timber buildings has grown significantly over the past two decades (Svatoš-Ražnjević et al., 2022). One of the primary drivers of this trend is the potential of timber structures to reduce carbon emissions within the construction industry (Churkina et al., 2020). Given the increasing scale and complexity of modern timber structures, achieving adequate ductility is essential. Ductile behavior may provide warning to the occupants through visible deformations prior to failure and enables load redistribution between structural members. Furthermore, it facilitates energy dissipation in case of seismic events (Jorissen and Fragiacomo, 2011) and increases the overall system reliability (Gollwitzer and Rackwitz, 1990). Contrary to steel and reinforced concrete, the primary failure modes of the timber members are brittle. Consequently, the ductility of timber structures should be provided through the connections (Ottenhaus et al., 2021). Glued-in plate connections are highly effective if large stiffness and capacity are required (Vallée et al., 2011; Bathon et al., 2014). However, their primary failure mode, which is the pull-out of the steel plate following timber shear failure along the adhesive, is inherently brittle. In this paper, we present a capacity-based design approach of glued-in steel plates in timber members that enforce a hierarchical organization of the failure modes using methods from system reliability. To prevent brittle plate pull-out, a ductile weak link was introduced by reducing the plate cross-section outside the timber member. A limit state function was then formulated to ensure this weak link yields before brittle pull-out occurs. The design of the weak link should account for the aleatoric uncertainties of both the steel and timber properties. Furthermore, the influence of the weak link on the overall connection capacity and stiffness should be considered. The capacity-based design approach with a hierarchical organization of the failure modes based on system reliability support the efficient and rational design of timber connections and structures.

2. Mechanical models

As depicted in Figure 1, a glued-in plate consists of a steel plate of cross-sectional area $w \cdot t_\mathrm{s}$ and elastic modulus E_s adhesively bonded into a timber member over a length l. The plate is perforated with holes on 40% of its area. The system was idealized as a double-lap shear joint with timber adherends of cross-sectional area $w \cdot t_\mathrm{t}$, elastic modulus E_t, and shear modulus G_t. The adhesive layer had a thickness t_a and shear modulus G_a. The weak link is located just outside the timber at the loaded end of the steel plate, by reducing the section t_w locally over a length l_w.

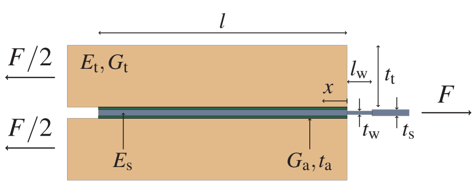

Figure 1. Schematic of a glued-in plate connection.

According to Tsai et al. (1998), the shear stress along the adhesive of a double-lap shear joint with finite shear rigidity of the timber adherends is:

$$\tau_\mathrm{a}(x) = A\sinh(\beta x) + B\cosh(\beta x), \quad (1)$$

with:

$$A = -\frac{1}{\beta\kappa^2}\frac{G_\mathrm{a}}{w t_\mathrm{a}}\frac{F}{E_\mathrm{s} t_\mathrm{s}}, \quad (2)$$

$$B = \frac{G_\mathrm{a} F\left(\frac{1}{2E_\mathrm{t}t_\mathrm{t}} + \frac{\cosh(\beta l)}{E_\mathrm{s}t_\mathrm{s}}\right)}{\beta\kappa^2 w t_\mathrm{a}\sinh(\beta l)}, \quad (3)$$

$$\beta^2 = \frac{\frac{G_\mathrm{a}}{t_\mathrm{a}}\left(\frac{2}{E_\mathrm{s}t_\mathrm{s}} + \frac{1}{E_\mathrm{t}t_\mathrm{t}}\right)}{1 + \frac{G_\mathrm{a}}{t_\mathrm{a}}\frac{t_\mathrm{t}}{3G_\mathrm{t}}} = \frac{\zeta^2}{\kappa^2}. \quad (4)$$

The constant β depends on the connection geometry and material properties, where ζ is the elongation parameter and κ the shear parameter. If the timber shear strength is governing, then the pull-out capacity is:

$$F_\mathrm{p,R} = \begin{cases} \text{if } \tau_\mathrm{a}(0) < \tau_\mathrm{a}(l) \\ \dfrac{f_\mathrm{v}\beta\kappa^2 w t_\mathrm{a}}{G_\mathrm{a}\frac{\cosh(\beta l)}{\sinh(\beta l)}\left(\frac{1}{2E_\mathrm{t}t_\mathrm{t}} + \frac{\cosh(\beta l)}{E_\mathrm{s}t_\mathrm{s}} - \frac{\sinh(\beta l)}{E_\mathrm{s}t_\mathrm{s}}\right)} \\ \text{else} \\ \dfrac{f_\mathrm{v}\beta\kappa^2 w t_\mathrm{a}\sinh(\beta l)}{G_\mathrm{a}\left(\frac{1}{2E_\mathrm{t}t_\mathrm{t}} + \frac{\cosh(\beta l)}{E_\mathrm{s}t_\mathrm{s}}\right)}. \end{cases} \quad (5)$$

The yield $F_\mathrm{y,R}$ and ultimate $F_\mathrm{u,R}$ capacities of the weak link are:

$$F_\mathrm{y,R} = A_\mathrm{w} f_\mathrm{y} = w t_\mathrm{w} f_\mathrm{y}, \quad (6)$$

$$F_\mathrm{u,R} = A_\mathrm{w} f_\mathrm{u} = w t_\mathrm{w} f_\mathrm{u}. \quad (7)$$

The plastic response of the weak link was modeled using Hollomon's power law (Hollomon, 1945) in terms of true stress and strain. This captures the strain hardening behavior up to the ultimate strain ϵ_u, which is essential for modeling the non-linear weak link displacement preceding the brittle pull-out failure $F_\mathrm{p,R}$. Finally, the tension capacity of the timber members is:

$$F_\mathrm{nt,R} = A_\mathrm{t} f_\mathrm{t,0} = w t_\mathrm{t} f_\mathrm{t,0}. \quad (8)$$

3. Reliability analysis

Random variables are mapped into the standard normal space by applying a Nataf transform (Nataf, 1962; Liu and Der Kiureghian, 1986). The reliability index β of the glued-in plate connections is evaluated using the first-order reliability method (FORM) (Rackwitz and Flessler, 1978). To determine the design parameters corresponding to a prescribed target reliability index, the inverse FORM algorithm by Der Kiureghian et al. (1994) is used.

3.1. *Limit state functions*

For each failure mode, the limit state functions are expressed in terms of the component capacities in Eqs. (5) to (8) and the design capacity P_d:

$$g_1(\mathbf{X}, \mathbf{c}) = F_\mathrm{p,R}(\mathbf{X}, \mathbf{c}) - P_\mathrm{d}, \quad (9)$$

$$g_{2\mathrm{a}}(\mathbf{X},\mathbf{c}) = F_{\mathrm{y,R}}(\mathbf{X},\mathbf{c}) - P_{\mathrm{d}}, \tag{10}$$

$$g_{2\mathrm{b}}(\mathbf{X},\mathbf{c}) = F_{\mathrm{u,R}}(\mathbf{X},\mathbf{c}) - P_{\mathrm{d}}, \tag{11}$$

$$g_{3}(\mathbf{X},\mathbf{c}) = F_{\mathrm{nt,R}}(\mathbf{X},\mathbf{c}) - P_{\mathrm{d}}, \tag{12}$$

where $\mathbf{X}$ is a vector of random variables and $\mathbf{c}$ is a vector of deterministic design parameters. To ensure a hierarchical calibration of the failure modes to provide ductility to the connection, the yield capacity of the weak link $F_{\mathrm{y,R}}$ should be lower than the plate pull-out capacity $F_{\mathrm{p,R}}$, which can be defined by:

$$g_{\mathrm{h}}(\mathbf{X},\mathbf{c}) = F_{\mathrm{p,R}}(\mathbf{X},\mathbf{c}) - F_{y,R}(\mathbf{X},\mathbf{c}). \tag{13}$$

3.2. *Connection reliability model*

The glued-in plate connection is modeled as a series system, following the Weibull weakest link theory (Weibull, 1939). The probability of pull-out failure $P_{\mathrm{f,p}}$ and the probability of timber tension failure $P_{\mathrm{f,nt}}$ are correlated since they both depend on the mechanical properties of timber. The probability of failure of the weak link $P_{\mathrm{f,u}}$ is not correlated with the other failure modes. By using Ditlevsen's bounds (Ditlevsen, 1979) and assuming small probabilities, the system probability of failure can be simplified to:

$$P_{\mathrm{f,sys}} = P_{\mathrm{f,p}} + P_{\mathrm{f,u}} + P_{\mathrm{f,nt}} - P_{\mathrm{f,pt}}. \tag{14}$$

$P_{\mathrm{f,pt}}$ is the joint probability of pull-out and tension failure:

$$P_{\mathrm{f,pt}} = \Phi_2(-\beta_{\mathrm{p}}, -\beta_{\mathrm{nt}}; \rho_{\mathrm{pt}}), \tag{15}$$

where Φ_2 is the bivariate standard normal cumulative distribution function, β_{p} is the reliability index for the steel pull-out failure, and β_{nt} is the reliability index corresponding to the timber tension failure. ρ_{pt} is the correlation between the two failure modes. This can be approximated as (Ditlevsen, 1979):

$$\begin{aligned} P_{\mathrm{f},ij} \approx \Phi(-\beta_i)\Phi\left(-\frac{\beta_j - \rho_{ij}\beta_i}{\sqrt{1-\rho_{ij}^2}}\right) \\ + \Phi(-\beta_j)\Phi\left(-\frac{\beta_i - \rho_{ij}\beta_j}{\sqrt{1-\rho_{ij}^2}}\right), \end{aligned} \tag{16}$$

where $\Phi(\cdot)$ is the cumulative standard normal distribution.

Finally, the system reliability index becomes:

$$\beta_{\mathrm{sys}} = -\Phi^{-1}(P_{\mathrm{f,sys}}). \tag{17}$$

3.3. *Target reliability indices*

The target reliability index for the connection was set to $\beta_{\mathrm{t}} = 3.8$, corresponding to a structure in consequence class 2 for a reference period of 50 years (CEN, 2002). Systems with multiple failure modes typically require higher component reliability to reach similar failure probability (Joint Committee on Structural Safety, 2000; Vrouwenvelder et al., 2024). This requirement is explicitly addressed in this study by ensuring that the target reliability is met at the connection-system level, rather than at the individual component level. Furthermore, the failure modes are organized in a hierarchy, such that the ductile weak link failure occurs first to ensure the connection ductility. To control this failure hierarchy, we introduced the hierarchical target reliability index β_{h}, which is directly related to the limit state function in Eq. (13).

3.4. *Input parameters*

The connection analyzed in this study consisted of an S355 steel plate with thickness $t_{\mathrm{s}} = 8$ mm that is adhesively embedded inside a square GL28h glued laminated timber member parallel to the grain with width $w = 120$ mm and thickness $t_{\mathrm{t}} = 54$ mm. The adhesive is epoxy-based with shear modulus $G_{\mathrm{a}} = 1400$ MPa (Almutairi, 2024) and bond thickness $t_{\mathrm{a}} = 2$ mm. Several glued-in lengths l and weak link thicknesses t_{w} and lengths l_{w} were studied. The deterministic input vector $\mathbf{c}$ contains the connection geometry, the design capacity P_{d} and the adhesive shear modulus G_{a}:

$$\mathbf{c} = (t_{\mathrm{s}}, t_{\mathrm{t}}, G_{\mathrm{a}}, t_{\mathrm{a}}, l, w, t_{\mathrm{w}}, P_{\mathrm{d}})^T. \tag{18}$$

As a simplification the geometry input parameters and the design capacity P_{d} were assumed deterministic and the latter was calibrated to match the target reliability β_{t}. The adhesive shear modulus G_{a} was also considered deterministically considering its negligible effect on the connection capacity and stiffness. The probabilistic input vector

Table 1. Statistical distributions and parameters for the material properties of steel (Joint Committee on Structural Safety, 2002; CEN, 2022) and timber (Schilling et al., 2021).

Variable	Distribution	Parameters
E_{t}	$\mathcal{LN}(\mu, cov)$	(14.0 GPa, 4.87 %)
G_{t}	$\mathcal{LN}(\mu, cov)$	(650 MPa, 5.13 %)
f_{v}	$\mathcal{W}(\mu, cov)$	(4.37 MPa, 14.3 %)
$f_{\mathrm{t,0}}$	$\mathcal{LN}(\mu, cov)$	(30.8 MPa, 11.0 %)
E_{s}	$\mathcal{LN}(\mu, cov)$	(210 GPa, 3.00 %)
f_{y}	$\mathcal{LN}(\mu, cov)$	(388 MPa, 7.00 %)
f_{u}	$\mathcal{LN}(\mu, cov)$	(735 MPa, 4.00 %)
ϵ_{u}	$\mathcal{LN}(\mu, cov)$	(0.12, 6.00 %)

X includes timber and steel material properties, which distributions and moments are defined in Table 1 and the correlation matrix in Table 2.

Table 2. Material properties' correlation matrix according to Joint Committee on Structural Safety (2002).

	E_{t}	G_{t}	f_{v}	$f_{\mathrm{t,0}}$	E_{s}	f_{y}	f_{u}	ϵ_{u}
E_{t}	1.0	0.6	0.4	0.8	0.0	0.0	0.0	0.0
G_{t}	0.6	1.0	0.6	0.4	0.0	0.0	0.0	0.0
f_{v}	0.4	0.6	1.0	0.6	0.0	0.0	0.0	0.0
$f_{\mathrm{t,0}}$	0.8	0.4	0.6	1.0	0.0	0.0	0.0	0.0
E_{s}	0.0	0.0	0.0	0.0	1.0	0.0	0.0	0.0
f_{y}	0.0	0.0	0.0	0.0	0.0	1.0	0.75	-0.45
f_{u}	0.0	0.0	0.0	0.0	0.0	0.75	1.0	-0.60
ϵ_{u}	0.0	0.0	0.0	0.0	0.0	-0.45	-0.60	1.0

4. Results and Discussion

The calibrated weak link thickness t_{w} was computed for various values of the hierarchical target reliability β_{h} and glued-in length l by applying the inverse FORM algorithm on the limit state function g_{h}. As shown in Figure 2, the weak link thickness t_{w} is significantly influenced by the hierarchical target reliability β_{h}. The latter controls the separation between the lower tail of the pull-out capacity $F_{\mathrm{p,R}}$ and the upper tail of the weak link yield capacity $F_{\mathrm{y,R}}$. A higher hierarchical target reliability β_{h} imposes more separation between the failure modes, resulting in a weaker weak link. The influence of the hierarchical target reliability β_{h} on the weak link thickness t_{w} increases with longer glued-in plates and is explained by statistical size

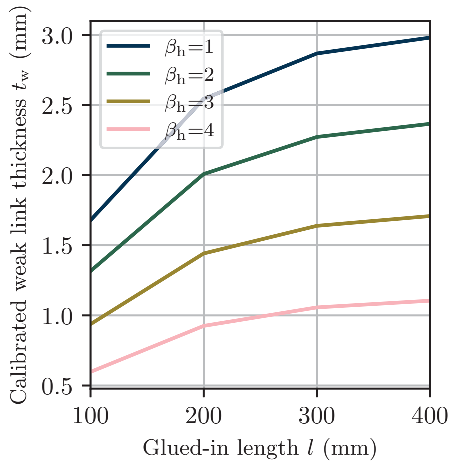

Figure 2. Calibrated weak link thickness t_{w} in function of the glued-in length l for various values of β_{h}.

effects. The size effects reflect the increased probability of encountering localized zones of lower strength as the bonded surface area extends. Independently of the hierarchical target reliability β_{h}, the pull-out capacity $F_{\mathrm{p,R}}$ increases with the glued-in length l until it reaches a plateau, which is directly reflected in the weak link thickness t_{w}.

To derive the design capacity P_{d}, steel failure can be defined either at the yield level $F_{\mathrm{y,R}}$ or at the ultimate level $F_{\mathrm{u,R}}$. As highlighted in Figure 3, this choice does not influence the design capacity P_{d} for a hierarchical target reliability β_{h} up to 3. This is because the pull-out capacity $F_{\mathrm{p,R}}$ governs the reliability of the design. Increasing β_{h} to 4 raises the separation between the limit states and leads to the yield capacity $F_{\mathrm{y,R}}$ being the governing component of the connection. In that case, considering the steel failure at the ultimate level drastically increases the design capacity of the connection.

The influence of the hierarchical target reliability β_{h} and the material properties on the connection reliability and ductility is shown in Figures (4) to (6) for a glued-in length of $l = 400$ mm. The relative contributions of the uncertainty in each variable X_i to the hierarchical reliability index β_h are quantified by the importance factors α_i^2. As depicted in Figure (4), the timber shear strength f_{v}

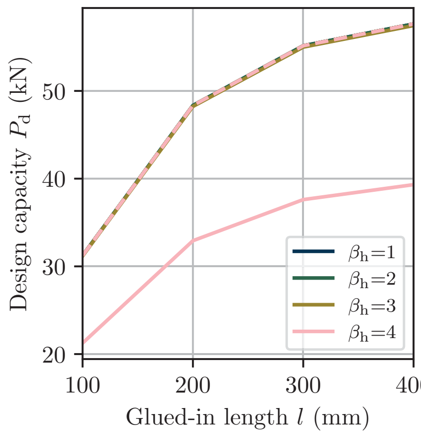

Figure 3. Connection design capacity P_d for various values of β_h. Steel failure is considered at the yield level (solid lines) and at the ultimate level (dashed lines).

accounts for almost all the uncertainty, followed by the steel yield strength f_y. Consequently, the probabilistic model for the timber shear strength f_v, and specifically its lower tail, almost exclusively drives the weak link thickness t_w. The probabilistic model for f_v should therefore be selected with great care. The elastic and shear moduli $E_{\{\mathrm{s,t}\}}$ and shear modulus G_t of the adherends provide negligible contributions and could be treated deterministically.

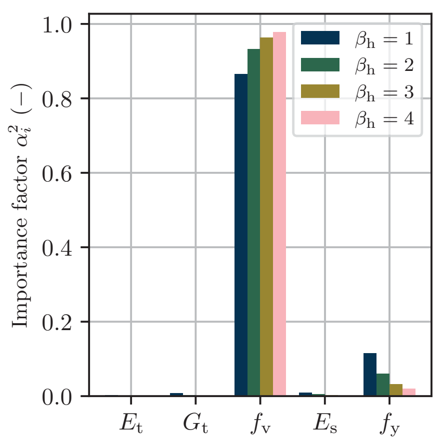

Figure 4. Importance factors α_i^2 for the parameters of the limit state function (13), used for the hierarchical calibration of the failure modes ($l = 400$ mm).

Figure 5 shows the normalized probability density of the capacity of the different connection components for two hierarchical reliability indices $\beta_\mathrm{h} = 2$ and $\beta_\mathrm{h} = 3$. The capacities $F_\mathrm{y,R}$, $F_\mathrm{u,R}$, and $F_\mathrm{nt,R}$ each depend on a single random variable and are represented as probabilistic models. Monte Carlo simulations with 10^5 samples were performed to generate the normalized probability density histogram for the pull-out capacity $F_\mathrm{p,R}$. Due to the higher variation in the timber mechanical properties, the scatter of the pull-out capacity $F_\mathrm{p,R}$ is significantly larger than the steel capacity at yield $F_\mathrm{y,R}$ and ultimate level $F_\mathrm{u,R}$. For the latter, distributions associated with lower β_h values and higher weak link thickness t_w exhibit greater dispersion, as absolute uncertainty scales proportionally with the mean resistance. The statistical interference between the pull-out capacity $F_\mathrm{p,R}$ and the yield capacity $F_\mathrm{y,R}$ corresponds to $P_\mathrm{f,h}$. This value quantifies the probability that the brittle failure precedes the ductile yield, thereby violating the intended hierarchy. Figure 5 clearly highlights how the hierarchical target reliability β_h controls the separation between the distribution of the pull-out capacity $F_\mathrm{p,R}$ and yield capacity $F_\mathrm{y,R}$. A higher hierarchical target reliability β_h corresponds to a lower $P_\mathrm{f,h}$, imposing less interference and more separation between the distributions. The pronounced lower tail of the pull-out capacity's distribution contributes significantly to the reduction of the weak link thickness t_w and the connection design capacity P_d. However, the large scatter of the pull-out capacity $F_\mathrm{p,R}$ enables the addition of a weak link without altering the connection design capacity P_d. The significant lower tail of the pull-out capacity $F_\mathrm{p,R}$ governs the connection design capacity P_d, even with a hierarchical target reliability $\beta_\mathrm{h} = 3$. This explains why the design capacity P_d was independent of the steel failure level for the hierarchical target reliability $\beta_\mathrm{h} \leq 3$ in Figure (3).

The hierarchical target reliability β_h controls the probability of the failure modes' hierarchy but cannot be used directly to quantify the connection ductility, which also depends on the weak link

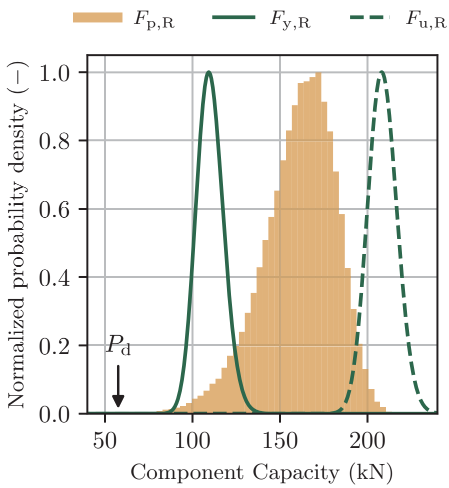

(a) $\beta_{\mathrm{h}} = 2$

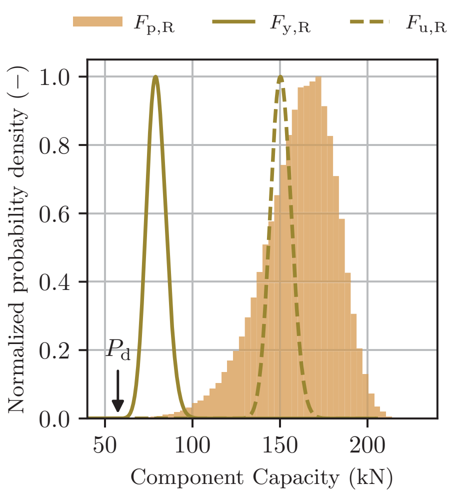

(b) $\beta_{\mathrm{h}} = 3$

Figure 5. Capacity distribution of the connection components for glued-in length $l = 400$ mm and various values of the hierarchical target reliability β_{h}. The distribution of the timber tensile capacity $F_{\mathrm{nt,R}}$ is not shown as its value is significantly higher than the other components.

geometry and its mechanical properties. As noted by Jorissen and Fragiacomo (2011) and Ottenhaus et al. (2021), the literature presents various definitions for timber connection ductility. In this study, ductility is defined as the ratio of the connection ultimate displacement to the connection yield displacement: $\mu = \delta_{\mathrm{u}}/\delta_{\mathrm{y}}$. Ductility is essential for failure warning, force redistribution, and energy dissipation. Since these effects depend mainly on the expected behavior of the structure, the connection load-displacement relationship was evaluated using mean material properties. The resulting curves for various values of the hierarchical target reliability β_{h} and weak link length l_{w} are shown in Figure (6). The hierarchical target reliability

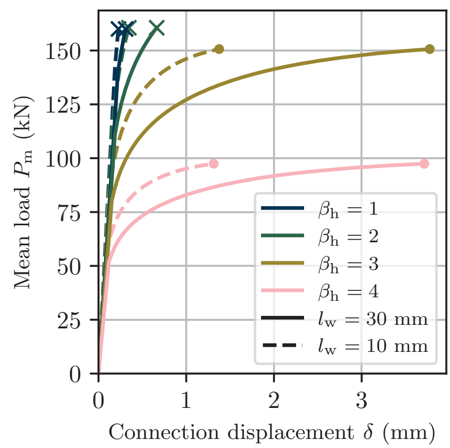

Figure 6. Connection load-displacement relation at the mean level for $l = 400$ mm and various values of the hierarchical target reliability β_{h} and weak link length l_{w}. Pull-out failures are indicated with the symbol $\times$ and steel failures with the symbol $\bullet$.

β_{h} strongly influences the connection mean load and displacement at failure. As β_{h} increases, the separation between the yield capacity $F_{\mathrm{y,R}}$ and pull-out capacity $F_{\mathrm{p,R}}$ increases, leading to higher deformation of the weak link when the pull-out capacity is reached. If the pull-out capacity exceeds the ultimate capacity of the weak link, the full potential of the weak link is used. Otherwise, the connection ductility is limited by a pull-out failure. Increasing the length of the weak link l_{w} results in a higher connection displacement at failure, meaning that it serves as a key design parameter to achieve the desired displacement or ductility ratio. However, lengthening the weak link also reduces the initial connection stiffness EA/L. Therefore, a balance must be found between ductility and stiffness.

A simpler design based on mean values would fail to provide a reliable hierarchical failure. Setting $\bar{F}_{\mathrm{y,R}} = \bar{F}_{\mathrm{p,R}}$ results in nearly a $50~\%$ probability of brittle pull-out failure before yielding even begins. Alternatively, $\bar{F}_{\mathrm{u,R}} = \bar{F}_{\mathrm{p,R}}$ only ensures a $50~\%$ probability that the weak link reaches its ultimate displacement, while remaining blind to the number of brittle pull-out failures that occur before yielding. Quantifying ductility at the mean level provides an estimate of the expected behavior of the connection. Nevertheless, when assessing the connection safety, it remains crucial to control the probability that yield precedes brittle pull-out failure. The hierarchical target reliability index β_{h} is an appropriate tool to quantify this margin. While defining a universal target β_{h} is difficult as it depends on the connection geometry, material properties, and the ductility demand, it provides a rational framework for performance-based capacity design.

Establishing a target hierarchical reliability index β_{h} requires a shift from the connection level to a building-level risk analysis. Within this framework, the probability and consequences of a progressive collapse must be weighted against the socio-economic costs incurred in achieving this target hierarchical reliability index β_{h}. For instance, while an increased β_{h} might enhance connection ductility and global system reliability, it may simultaneously reduce the connection design capacity P_{d} and stiffness. This reduction influences structural efficiency and directly affects the cost-effectiveness and sustainability of the building. However, a target hierarchical reliability index β_{h} can contribute to rational and targeted measures to increase the robustness of a building.

5. Conclusion and Outlook

The hierarchical target reliability index and inverse first-order reliability methods enable the control and calibration of failure modes within a performance-based capacity design framework. We demonstrated this on timber connections comprising glued-in plates. Furthermore, this framework facilitates the design of the weak link, the assessment of the connection ductility, and the determination of the design capacity. For connections with glued-in plates, a steel weak link can be introduced to provide ductility without reducing the overall capacity of the connection significantly. This is attributed to the lower uncertainty of steel mechanical properties relative to timber. However, these findings rely on the validity of the underlying probabilistic model for the timber shear strength and the mechanical model for the pull-out capacity, which may carry some ambiguities. Consequently, further experimental validation is required alongside further investigations to establish appropriate methods for selecting the hierarchical target reliability index across various structures.

Acknowledgement

The authors gratefully acknowledge the financial support provided by Innosuisse - Swiss Innovation Agency (Project No. 108.248 IP-ENG) and the project partner, Hilti AG.

References

Almutairi, A. D. (2024). Comprehensive Investigation of Epoxy Adhesives for Structural Applications in Saudi Arabia: Mechanical Performance, Environmental Impacts, and Analysis on Health. *Polymers 16*(22), 3185.

Bathon, L., O. Bletz-Mühldorfer, F. Diehl, J. Schmidt, A. Wagner, and M. Weil (2014). Anwendungen von eingeklebten Lochblechen unter statischen sowie ermüdenden Einwirkungen. In *Proceedings of the 20 Internationales Holzbau-Forum IHF*.

CEN (2002). Eurocode 0: Basis of structural design.

CEN (2022). Eurocode 3 - Design of steel structures - Part 1-1: General rules and rules for buildings.

Churkina, G., A. Organschi, C. P. O. Reyer, A. Ruff, K. Vinke, Z. Liu, B. K. Reck, T. E. Graedel, and H. J. Schellnhuber (2020, January). Buildings as a global carbon sink. *Nature Sustainability 3*(4), 269–276.

Der Kiureghian, A., Y. Zhang, and C. Li (1994). Inverse Reliability Problem. *Journal of Engineering Mechanics 120*(5), 1154–1159.

Ditlevsen, O. (1979). Narrow Reliability Bounds for Structural Systems. *Journal of Structural Mechanics 7*(4), 453–472.

Gollwitzer, S. and R. Rackwitz (1990). On the reliability of Daniels systems. *Structural Safety 7*(2-4), 229–243.

Hollomon, J. H. (1945). Tensile deformation. *Aime Trans 12*, 1–22.

Joint Committee on Structural Safety (2000). JCSS Probabilistic Model Code (PMC) - Part I - Basis of Design.

Joint Committee on Structural Safety (2002). JCSS Probabilistic Model Code (PMC) - Part III - Resistance models.

Jorissen, A. and M. Fragiacomo (2011). General notes on ductility in timber structures. *Engineering Structures 33*(11), 2987–2997.

Liu, P.-L. and A. Der Kiureghian (1986). Multivariate distribution models with prescribed marginals and covariances. *Probabilistic Engineering Mechanics 1*(2), 105–112.

Nataf, A. (1962). Détermination des distributions de probabilités dont les marges sont données. *Comptes Rendus de l'Académie des Sciences 225*, 42–43.

Ottenhaus, L.-M., R. Jockwer, D. Van Drimmelen, and K. Crews (2021). Designing timber connections for ductility – A review and discussion. *Construction and Building Materials 304*, 124621.

Rackwitz, R. and B. Flessler (1978). Structural reliability under combined random load sequences. *Computers & Structures 9*(5), 489–494.

Schilling, S., P. Palma, R. Steiger, and A. Frangi (2021). Probabilistic description of the mechanical properties of glued laminated timber made from softwood. In *INTER Proceedings Meeting Fifty-Four 2021*, pp. 333–349.

Svatoš-Ražnjević, H., L. Orozco, and A. Menges (2022). Advanced Timber Construction Industry: A Review of 350 Multi-Storey Timber Projects from 2000–2021. *Buildings 12*(4), 404.

Tsai, M., D. Oplinger, and J. Morton (1998). Improved theoretical solutions for adhesive lap joints. *International Journal of Solids and Structures 35*(12), 1163–1185.

Vallée, T., T. Tannert, and S. Hehl (2011). Experimental and numerical investigations on full-scale adhesively bonded timber trusses. *Materials and Structures 44*(10), 1745–1758.

Vrouwenvelder, T., S. Dimova, L. M. Sousa, J. Marková, G. Mancini, and et al. (2024). *Reliability background of the Eurocodes: support to the implementation, harmonization and further development of the Eurocodes*. Luxembourg: Publications Office of the European Union.

Weibull, W. (1939). A statistical theory of the strength of materials. *Transactions of The Royal Swedish Institute for Engineering Sciences 151*.